

# Mechanical properties of homogeneous and heterogeneous layered 2D materials

Robert M. Elder\*, Mahesh R. Neupane\*, and Tanya L. Chantawansri

Macromolecular Science & Technology Branch  
U.S. Army Research Laboratory  
Aberdeen Proving Ground, MD

\* corresponding authors: robert.elder26.ctr@mail.mil; mahesh.neupane.ctr@mail.mil

**Abstract**—Transition metal dichalcogenides (TMDC) such as molybdenum disulfide ( $\text{MoS}_2$ ) are 2D materials that are promising for flexible electronics and piezoelectric applications, but their low mechanical strength limits practical use. In this work, we study the mechanical properties of heterostructures containing  $\text{MoS}_2$  and graphene, another 2D material with exceptional mechanical properties, using atomistic molecular dynamics simulations of nanoindentation. We consider bi- and tri-layer heterostructures where graphene either supports or encapsulates  $\text{MoS}_2$ , and we compare to the monolayers and homogeneous bilayers. We extract mechanical properties (Young's modulus) from nanoindentation simulations. All of the heterostructures have larger Young's moduli than the mono- and bi-layer  $\text{MoS}_2$ , demonstrating that graphene provides mechanical reinforcement regardless of layer stacking order. Our results demonstrate the potential of heterostructures to improve the mechanical properties of TMDC materials, which would increase their utility for device applications.

**Keywords**—mechanical properties; 2D materials; molecular dynamics simulation

## I. INTRODUCTION

Two-dimensional (2D) materials such as graphene and molybdenum disulfide ( $\text{MoS}_2$ ) are at the forefront of industrial and academic research, owing to their unique electronic, mechanical, thermal, and optical properties. Although graphene and  $\text{MoS}_2$  possess a similar in-plane hexagonal lattice structure, their lattice structures out-of-plane are quite different. Graphene contains  $\text{sp}^2$ -bonded carbon atoms, while  $\text{MoS}_2$  constitutes a tetragonally aligned tri-layer between a transition metal (Mo) atom and two chalcogenide (S) atoms. As a result, the electronic and mechanical properties of graphene and  $\text{MoS}_2$  are significantly different. Pristine graphene is metallic and mechanically stronger than steel, with a Young's modulus of  $\sim 1$  TPa [1]. In contrast,  $\text{MoS}_2$  is a semiconductor and is useful in device applications, but has Young's modulus of only about 0.25 TPa [2]. Recently, there have been efforts to combine these two materials for applications such as ultra-gain photodetectors [3], thermal interface materials [4], and superlubric materials [5]. Developing a deeper understanding of the electronic and mechanical properties of these heterostructures is critical for extending their applicability into other exotic applications such

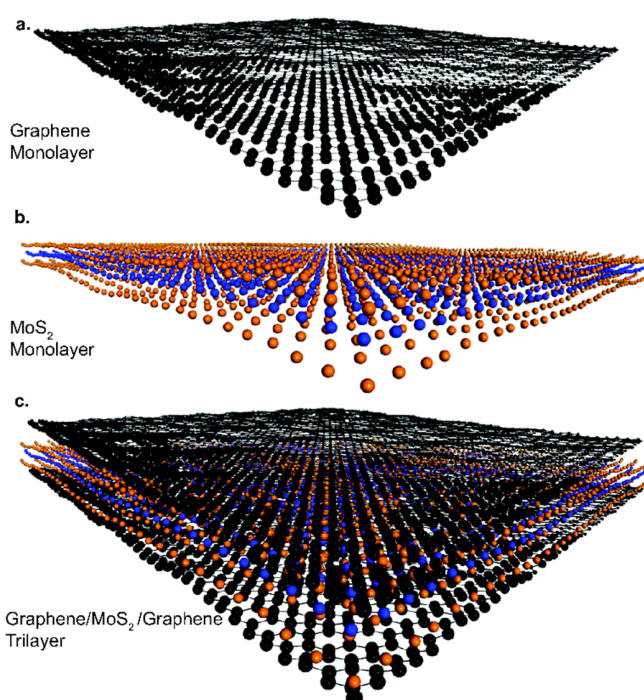


Fig. 1. Atomistic schematics of a) graphene (G) and b)  $\text{MoS}_2$  (M) monolayers, and c) a graphene- $\text{MoS}_2$ -graphene (G/M/G) trilayer heterostructure. Carbon, molybdenum, and sulfur atoms are colored black, blue, and orange, respectively.

as excitonic, spintronics, and piezoelectric applications. In particular, piezoelectric applications demand a systematic study on how the mechanical properties depend on the layer stacking order. In this study, we use atomistic molecular dynamics simulations to study the mechanical deformation of graphene/ $\text{MoS}_2$  heterostructures with various stacking patterns relative to both single layers and homogeneous bilayers.

To mimic experimental methods for measuring the mechanical properties of 2D materials [1], we conduct simulated nanoindentation of several 2D homogeneous and heterogeneous systems. These systems are monolayers of either graphene (G) or  $\text{MoS}_2$  (M), bi-layers of graphene (G/G) or  $\text{MoS}_2$  (M/M), bi-

layer heterostructures with both graphene and MoS<sub>2</sub> (G/M and M/G), and tri-layer sandwich heterostructures (G/M/G and M/G/M).

## II. MODELS AND METHODS

To construct single- and multi-layer models for the indentation study (Fig. 1), we obtained optimized structure parameters of the single layers from first-principle calculations performed using VASP tools [6, 7]. Using the Perdew-Burke-Ernzerhof (PBE) form of generalized-gradient approximation (GGA) [8, 9], optimized parameters for single layer graphene ( $a = 2.46 \text{ \AA}$ ) and MoS<sub>2</sub> ( $a = 3.179 \text{ \AA}$  and  $c = 12.729 \text{ \AA}$ ) were obtained.

Using the DFT-generated lattice parameters, we constructed single layer, bilayer, and trilayer planar models as shown in the Fig. 1. We performed atomistic molecular dynamics (MD) simulations using LAMMPS (<http://lammmps.sandia.gov>) [15]. The interatomic interactions for MoS<sub>2</sub> were described by a Stillinger-Weber potential, while carbon-carbon interactions in graphene were described by a bond-order potential with built-in long-range corrections (LCBOP) [16, 17]. The weak inter-layer van der Waals (vdW) interactions between MoS<sub>2</sub> layers were described by a Lennard-Jones (L-J) potential with energy and distance parameters  $\epsilon = 6.93 \text{ meV}$  and  $\sigma = 3.13 \text{ \AA}$  [16, 18]. In heterostructures, graphene and MoS<sub>2</sub> layers were coupled by vdW interactions, which were described using a L-J potential with  $\epsilon = 3.95 \text{ meV}$  and  $\sigma = 3.625 \text{ \AA}$ , respectively [19]. The integration time step was 0.5 fs. L-J interactions were cut off at 10  $\text{\AA}$ .

Prior to indentation simulations, all models were equilibrated using the following procedure. First, a small ( $\sim 3 \text{ nm}^2$ ) material system was constructed with the surface normal to the  $z$ -dimension. The energy was minimized using steepest descent and conjugate gradient minimization, each for  $10^4$  steps, to remove highly unfavorable atomic interactions. The small system was then equilibrated during 100 picoseconds ( $ps$ ) of constant temperature-constant pressure ( $NPT$ ) MD at 300 K and 1 atm using the Nosé-Hoover thermostat and barostat with damping constants of 20 and 200 femtoseconds ( $fs$ ), respectively [10]. The barostat acted independently on the  $x$ - and  $y$ -dimensions and the  $xy$  tilt factor. The small system was then replicated in the  $xy$ -plane to yield a large system of about  $75 \times 75 \text{ nm}^2$ , which was subsequently equilibrated for another 50  $ps$ . Following this final equilibration, a circular section with radius  $a = 30 \text{ nm}$  was identified in the center of the large system. Atoms within this radius were free to move during nanoindentation, while atoms outside this radius were clamped in place to form a rigid boundary. The 30 nm radius is comparable to previous simulation studies [11]. This simulation design mimics experimental methods for measuring the mechanical properties of 2D materials [1].

Following the above procedure, we obtained the force exerted on the 2D materials as a function of indentation depth (i.e., deflection,  $\delta$ ). A spherical indenter was assumed and described by a purely repulsive harmonic potential,  $F(r) = k(r-R)^2$ , where  $F$  is the force on an atom at a distance  $r$  from the indenter with radius  $R$  (10 nm, similar to previous simulation and experimental studies) [1, 11], and  $k$  is the force constant ( $217 \text{ meV/\AA}^3 \approx 5 \text{ kcal/mol/\AA}^3$ ). The force was zero for

$r > R$ . Initially, we positioned the indenter in the center of the circular section with a vertical spacing of  $\sim 2 \text{ \AA}$  between the indenter tip and the surface. The indenter was then lowered into the material at a speed of  $0.5 \text{ \AA/ps}$ , similar to previous simulation studies [11]. The force was then calculated as the total normal force on the spherical indenter. We define indentation depth ( $\delta$ ) as the difference between the initial position of the center-of-mass of the material and the lowest point of the indenter. During indentation, constant volume-constant temperature ( $NVT$ ) MD was employed, where the temperature of the atoms inside the circular section was maintained at 300 K using the thermostat described above.

Intrinsic mechanical properties were then calculated by fitting the force ( $F$ )-deflection ( $\delta$ ) curves to the following relation [1, 12].

$$F(\delta) = c\delta + d\delta^3 \quad (1)$$

The thickness-normalized Young's modulus  $E^{2D}$  and pre-tension  $\sigma_0$  of a membrane with thickness  $h$  can then be determined from the fitting coefficients ( $c$ ,  $d$ ) using the relations  $c = \sigma_0 \pi h$  and  $d = E^{2D} q^3 a^2 h$ , where  $q = (1.05 - 0.15\nu - 0.16\nu^2)^{-1}$  is a dimensionless constant,  $\nu$  is the Poisson's ratio, and  $a$  is the hole radius. The Young's modulus of an equivalent bulk material,  $E$ , is calculated as  $E^{2D} h^{-1}$  [13]. For monolayer graphene and MoS<sub>2</sub>, we assume thicknesses of 0.335 nm and 0.609 nm, respectively [13], where the thickness of the multilayer structures are defined as the sum of the layer thicknesses. We use  $\nu = 0.165$  for graphene,  $\nu = 0.25$  for MoS<sub>2</sub>, and the weighted average of these values for multilayer structures [14]. Though these values of  $\nu$  are zeroth-order approximations, the dimensionless parameter  $q$  is relatively insensitive to  $\nu$ . We only fit (1) to the low-deflection ( $\delta \leq 10 \text{ nm}$ ) data [12].

## III. RESULTS AND DISCUSSION

Force ( $F$ )-deflection ( $\delta$ ) curves obtained from nanoindentation simulations are shown in Fig. 2.

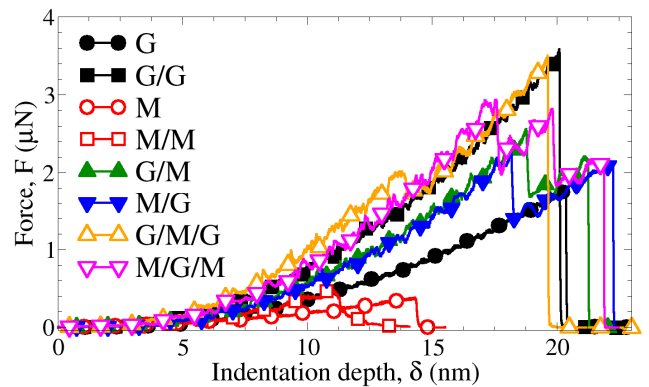


Fig. 2. Force ( $F$ )-deflection ( $\delta$ ) curves from simulated nanoindentation of 2D materials. G indicates a graphene layer, and M indicates a MoS<sub>2</sub> layer.

TABLE I. YOUNG'S MODULI OF 2D MONO-, BI-, AND TRI-LAYER SYSTEMS.

System	This study (TPa)	Literature values (TPa)
G	1.05	$1.0 \pm 0.1$ [1]
G/G	1.06	$1.04 \pm 0.1$ [20]
M	0.16	$0.27 \pm 0.1$ [21]
M/M	0.27	$0.2 \pm 0.1$ [21]
G/M	0.53	$0.49 \pm 0.05$ [14]
M/G	0.52	--
G/M/G	0.68	0.56 [19]
M/G/M	0.45	--

The force increases slowly up to deflections of about 5 nm, at which point the force increases quickly up to failure. In the homogeneous bilayer systems, while these structures support larger forces than their monolayer counterparts, the MoS<sub>2</sub> bilayer is punctured more easily than the graphene bilayer. The bilayer heterostructures show similar maximum forces as the graphene monolayer, but exhibit two force peaks that correspond to the failure of MoS<sub>2</sub> and graphene, respectively. The trilayer heterostructures have maximum forces approaching the graphene bilayer, and exhibit two or more force peaks, corresponding to the rupture of individual layers, with MoS<sub>2</sub> layers always failing before graphene layers.

The Young's moduli for the 2D materials are shown in Table 1. For homogeneous structures, we have excellent agreement with experimental values: the moduli for graphene and MoS<sub>2</sub> mono- and bi-layers are ~1 TPa and ~0.25 TPa, respectively. The G/M and M/G bilayer heterostructures both have moduli of ~0.5 TPa, demonstrating that graphene provides mechanical reinforcement regardless of layer ordering. The trilayer heterostructures can provide larger or smaller Young's moduli than the bilayers, depending on the MoS<sub>2</sub> content. The moduli of heterostructures can be estimated accurately using the weighted average of the moduli of the layers [19].

These results suggest that MoS<sub>2</sub>, supported or encapsulated by graphene to form bi- or tri-layer heterostructures, has superior mechanical properties compared with mono- and bi-layer MoS<sub>2</sub>. Since other 2D materials, such as MoSe<sub>2</sub>, WS<sub>2</sub>, and WSe<sub>2</sub>, have similar bonding and inter-layer vdW forces as MoS<sub>2</sub>, our observations and approach open new avenues for the design of more robust 2D materials and for the characterization of their mechanical strength through large-scale atomistic modeling, which complements experimental efforts.

#### ACKNOWLEDGMENTS

RME and MRN were supported by an appointment to the Postgraduate Research Participation Program at the U.S. Army Research Laboratory administered by the Oak Ridge Institute for Science and Education through an interagency agreement between the U.S. Department of Energy and USARL. This work was supported by grants of computer time from the DOD High Performance Computing Modernization Program at the U.S. Air

Force Research Laboratory and U.S. Army Engineer Research and Development Center DoD Supercomputing Resource Centers.

#### REFERENCES

- [1] C. Lee, X. Wei, J. W. Kysar, and J. Hone, "Measurement of the elastic properties and intrinsic strength of monolayer graphene," *Science*, vol. 321, pp. 385-388, 2008.
- [2] A. Castellanos-Gomez, M. Poot, G. A. Steele, H. S. J. van der Zant, N. Agrait, and G. Rubio-Bollinger, "Elastic Properties of Freely Suspended MoS<sub>2</sub> Nanosheets," *Adv. Mater.*, vol. 24, pp. 772-775, 2012.
- [3] W. Zhang, C.-P. Chuu, J.-K. Huang, C.-H. Chen, M.-L. Tsai, Y.-H. Chang, et al., "Ultrahigh-Gain Photodetectors Based on Atomically Thin Graphene-MoS<sub>2</sub> Heterostructures," *Sci. Rep.*, vol. 4, 2014.
- [4] B. Liu, F. Meng, C. D. Reddy, J. A. Baimova, N. Srikanth, S. V. Dmitriev, et al., "Thermal transport in a graphene-MoS<sub>2</sub> bilayer heterostructure: a molecular dynamics study," *R. Soc. Chem. Adv.*, vol. 5, pp. 29193-29200, 2015.
- [5] W. Lin-Feng, M. Tian-Bao, H. Yuan-Zhong, Z. Quanshui, W. Hui, and L. Jianbin, "Superlubricity of two-dimensional fluorographene/MoS<sub>2</sub> heterostructure: a first-principles study," *Nanotechnology*, vol. 25, p. 385701, 2014.
- [6] G. Kresse and J. Hafner, "Ab initio molecular dynamics for open-shell transition metals," *Phys. Rev. B: Solid State*, vol. 48, pp. 13115-13118, 1993.
- [7] G. Kresse and J. Furthmüller, "Efficiency of ab-initio total energy calculations for metals and semiconductors using a plane-wave basis set," *Comput. Mater. Sci.*, vol. 6, pp. 15-50, 1996.
- [8] J. P. Perdew, K. Burke, and M. Ernzerhof, "Generalized Gradient Approximation Made Simple," *Phys. Rev. Lett.*, vol. 77, pp. 3865-3868, 1996.
- [9] M. Ernzerhof and G. E. Scuseria, "Assessment of the Perdew-Burke-Ernzerhof exchange-correlation functional," *J. Chem. Phys.*, vol. 110, pp. 5029-5036, 1999.
- [10] W. Shinoda, M. Shiga, and M. Mikami, "Rapid estimation of elastic constants by molecular dynamics simulation under constant stress," *Phys. Rev. B: Solid State*, vol. 69, p. 134103, 2004.
- [11] Z. D. Sha, Q. Wan, Q. X. Pei, S. S. Quek, Z. S. Liu, Y. W. Zhang, et al., "On the failure load and mechanism of polycrystalline graphene by nanoindentation," *Sci. Rep.*, vol. 4, 2014.
- [12] X. Tan, J. Wu, K. Zhang, X. Peng, L. Sun, and J. Zhong, "Nanoindentation models and Young's modulus of monolayer graphene: A molecular dynamics study," *Appl. Phys. Lett.*, vol. 102, p. 071908, 2013.
- [13] J.-W. Jiang, "Graphene versus MoS<sub>2</sub>: A short review," *Front. Phys.*, pp. 1-16, 2015.
- [14] K. Liu, Q. Yan, M. Chen, W. Fan, Y. Sun, J. Suh, et al., "Elastic Properties of Chemical-Vapor-Deposited Monolayer MoS<sub>2</sub>, WS<sub>2</sub>, and Their Bilayer Heterostructures," *Nano Lett.*, vol. 14, pp. 5097-5103, 2014.
- [15] S. Plimpton, "Fast Parallel Algorithms for Short-Range Molecular Dynamics," *J. Comp. Phys.*, vol. 117, pp. 1-19, 1995.
- [16] J.-W. Jiang, H. S. Park, and T. Rabczuk, "Molecular dynamics simulations of single-layer molybdenum disulphide (MoS<sub>2</sub>): Stillinger-Weber parametrization, mechanical properties, and thermal conductivity," *J. Appl. Phys.*, vol. 114, p. 064307, 2013.
- [17] J. H. Los and A. Fasolino, "Intrinsic long-range bond-order potential for carbon: Performance in Monte Carlo simulations of graphitization," *Phys. Rev. B: Solid State*, vol. 68, p. 024107, 2003.
- [18] T. Liang, S. R. Phillpot, and S. B. Sinnott, "Parametrization of a reactive many-body potential for MoS<sub>2</sub> systems," *Phys. Rev. B: Solid State*, vol. 79, p. 245110, 2009.
- [19] J.-W. Jiang and H. S. Park, "Mechanical properties of MoS<sub>2</sub>/graphene heterostructures," *Appl. Phys. Lett.*, vol. 105, p. 033108, 2014.
- [20] C. Lee, X. Wei, Q. Li, R. Carpick, J. W. Kysar, and J. Hone, "Elastic and frictional properties of graphene," *Phys. Status Solidi B*, vol. 246, pp. 2562-2567, 2009.
- [21] S. Bertolazzi, J. Brivio, and A. Kis, "Stretching and Breaking of Ultrathin MoS<sub>2</sub>," *ACS Nano*, vol. 5, pp. 9703-9709, 2011.